Available online at www.sciencedirect.com
ScienceDirect
Quaternary Research 68 (2007) 239–248
QUATERNARY RESEARCH
www.elsevier.com/locate/yqres

Molar gas ratios of air entrapped in ice: A new tool to determine the origin of relict massive ground ice bodies in permafrost

Raphaelle Cardyn [a], Ian D. Clark [a], Denis Lacelle [a,*], Bernard Lauriol [b], Christian Zdanowicz [c], Fabrice Calmels [d]

[a] Department of Earth Sciences, University of Ottawa, 140 Louis Pasteur, Ottawa, ON, Canada K1N 6N5
[b] Department of Geography, University of Ottawa, 60 University St., Ottawa, ON, Canada K1N 6N5
[c] National Glaciology Programme, Geological Survey of Canada (NRCan), 601 Booth St., Ottawa, ON, Canada K1A 0E8
[d] Centre d'Études Nordiques, Université Laval, Sainte-Foy, QC, Canada G1K 7P4

Received 6 June 2006
Available online 23 July 2007

Abstract

The molar ratios of atmospheric gases change during dissolution in water due to differences in their relative solubilities. We exploited this characteristic to develop a tool to clarify the origin of ice formations in permafrost regions. Extracted from ice, molar gas ratios can distinguish buried glacier ice from intrasedimental ground ice formed by freezing groundwaters. An extraction line was built to isolate gases from ice by melting and trapping with liquid He, followed by analysis of N_2, O_2, Ar, $^{18}O_{O2}$ and $^{15}N_{N2}$, by continuous flow mass spectrometry. The method was tested using glacier ice, aufeis ice (river icing) and intrasedimental ground ice from sites in the Canadian Arctic. O_2/Ar and N_2/Ar ratios clearly distinguish between atmospheric gas in glacial ice and gases from intrasedimental ground ice, which are exsolved from freezing water. $\delta^{15}N_{N2}$ and $\delta^{18}O_{O2}$ in glacier ice, aufeis ice and intrasedimental ground ice do not show clear distinguishing trends as they are affected by various physical processes during formation such as gravitational settling, excess air addition, mixing with snow pack, and respiration.
© 2007 University of Washington. All rights reserved.

Keywords: Molar gas ratios; Glacier ice; Massive ground ice; Permafrost; Canadian Arctic

Introduction

According to the ACGR (1988), massive ground ice bodies consist of large tabular ice bodies whose volumetric ice content exceeds 95%, whereas icy sediments contain excess ice and have a volumetric ice content in the >50 to 95% range. In formerly glaciated permafrost regions, natural exposures of buried massive ground ice and icy sediments bodies (hereafter: MI/IS) may be observed in the headwall of thermokarst slumps and within eroded river banks and coastal cliffs. The nature and origin of these MI/IS bodies have been attributed to either a *glacial* origin, as firnified or basal ice (Lorrain and Demeur, 1985; Astakhov, 1986; Kaplyanskaya and Tarnogradski, 1986; French and Harry, 1990; St-Onge and McMartin, 1995; Dyke and Savelle, 2000), or *intrasedimental* ice of a segregation/intrusive origin (Mackay, 1966; 1971; Burn et al., 1986; Harry et al., 1988; Pollard, 1991; Mackay and Dallimore, 1992; Lacelle et al., 2004; Murton et al., 2005). The burial of glacial ice occurs when sediments are deposited on top of the ice or when debris melts out from the basal ice, forming an insulating blanket of supraglacial debris. If the thickness of the sediments covering the ice eventually exceeds that of the active layer (top layer of soil that undergoes seasonal freeze/thaw), the ice can be preserved indefinitely. Alternatively, massive segregated-intrusive ice bodies tend to occur within the subglacial and/or proglacial permafrost where pressurized glacial meltwater freezes onto the base of permafrost, or if permafrost aggrades through previously thawed sediments upon exposure to cold air following the retreat of glaciers (e.g., Rampton, 1988). Determining the origin of MI/IS bodies has important implications regarding the dynamics of ice sheets and for geomorphological, paleoclimatic and paleoenvironmental reconstructions.

* Corresponding author. Current address: Canadian Space Agency, 6767 route de l'aeroport, St-Hubert, QC, Canada J3Y 8Y9. Fax: +1 450 926 4766.
E-mail addresses: rcardyn@isotrace.co.nz (R. Cardyn), idclark@uottawa.ca (I.D. Clark), denis.lacelle@space.gc.ca (D. Lacelle), blauriol@uottawa.ca (B. Lauriol), czdanowi@nrcan.gc.ca (C. Zdanowicz), fabrice.calmels.1@ulaval.ca (F. Calmels).

0033-5894/$ - see front matter © 2007 University of Washington. All rights reserved.
doi:10.1016/j.yqres.2007.05.003

https://doi.org/10.1016/j.yqres.2007.05.003 Published online by Cambridge University Press

To date, several approaches have been used to attempt to definitely characterize the origin of MI/IS in permafrost. For example, the textural and morphological context of the massive ground ice bodies and their relation with adjacent sediments (Murton and French, 1994; Murton et al., 2004; Murton, 2005), the crystallographic characteristics (French and Pollard, 1986; Pollard, 1991), chemical composition (Leibman, 1996) and stable isotope of oxygen and hydrogen of the ice (Lorrain and Demeur, 1985; Mackay and Dallimore, 1992; Lacelle et al., 2004) have all been employed to attempt to distinguish between buried glacial and intrasedimental ice. However, none of these methods, when used alone, unambiguously distinguish between buried glacial ice and segregated-intrusive ground ice bodies. For example, in the western Canadian Arctic, the massive ground ice exposure at Peninsula Point displays characteristics that could be indicative of buried glacier ice or segregated ice, but since the massive ice is located beyond the limits of Pleistocene glaciation, a glacier ice origin cannot be accepted (Mackay and Dallimore, 1992). Similar ambiguous observations were also recorded from the massive ice exposures in the eastern Siberia, Russia (Astakhov, 1986; Kaplyanskaya and Tarnogradski, 1986; Leibman, 1996).

One approach that has been used with success to determine the origin of MI/IS bodies in permafrost is the analysis of the concentration and $\delta^{13}C$ value of CO_2 gases occluded within the ground ice body (Moorman et al., 1998; Lacelle et al., 2004). The concentration of CO_2 entrapped in ice can distinguish between glacier and intrasedimental ice because in the latter, CO_2 concentration is expected to be 10 to 100 times greater than atmospheric values due to the oxidation of organic carbon to CO_2 by microbial activity in soils. However, not many studies have employed this technique due to the complications in returning unthawed ice samples back to the laboratory.

Since the molar ratios of atmospheric gases change during dissolution in water due to differences in their relative solubilities, a potential new approach to determine the origin of MI/IS bodies is the measurement of the relative abundances of O_2, N_2 and Ar gases entrapped in ice and their stable isotope ratios. The objective of this study is therefore to determine whether the molar gas ratios (N_2/Ar, O_2/Ar), $\delta^{18}O_{O2}$ and $\delta^{15}N_{N2}$ can be used as a new diagnostic tool to determine the origin of MI/IS in permafrost. In this study, the theory surrounding the use of the relative abundances of O_2, N_2 and Ar gases entrapped in ice as a diagnostic tool is first presented, followed by some measurements from glacier ice, aufeis ice and massive ground ice bodies of segregated-intrusive origins.

Background on the origin of gases entrapped in ice

Gases entrapped in glacier ice

The gas composition of the atmosphere is dominated by N_2 (78.08%), followed by O_2 (20.94%) and Ar (0.93%). This produces O_2/Ar and N_2/Ar ratios of 22.42 and 83.60, respectively, with little change over time. In glacier ice, atmospheric gases are trapped through the process of firn densification and occlusion of porosity (Craig et al., 1988; Sowers et al., 1992; Schwander, 1996). The complete occlusion of air in the ice can take several years and as a consequence, the gases trapped in the ice can be much younger than the ice itself (Barnola et al., 1991; Arnaud et al., 2000; Clark et al., 2007).

During occlusion of the gases in the firn layer, the relative abundance of O_2, N_2 and Ar gases and $\delta^{18}O_{O2}$ and $\delta^{15}N_{N2}$ entrapped in glacier ice can be slightly modified from the initial atmospheric values. For example, the molar ratios of gases trapped in glacier ice are mainly affected by gravitational fractionation and the presence of micro-fissures in the ice. Gravitational fractionation of heavy gases, such as Ar, relative to lighter gases like O_2 during occlusion of the gases in the firn can lead to a decrease in the O_2/Ar and N_2/Ar ratios. The magnitude of the latter is determined by the structure of the firn, which is influenced by temperature, wind speed and snow accumulation rate at the depositional site (Hattori, 1983; Mariotti, 1983; Sowers and Bender, 1989; Caillon et al., 2003; Landais et al., 2006; Petrenko et al., 2006).

The presence of micro-fractures in the ice can also affect molar gas ratios of the gases entrapped in the ice. If there are micro-fractures in the ice, the smaller atoms of Ar will diffuse faster than the molecules of O_2 and N_2, with larger cross-sectional diameter (Craig et al., 1988). On the other hand, the isotopic composition of the gases entrapped in the ice is mainly affected by thermo-fractionation. The $\delta^{18}O_{O2}$ can provide an indication of rapid temperature changes as it is influenced by changes in the measured $\delta^{18}O$ of ocean water, which reflects global changes in ice volume (Bender et al., 1994). Since the late Pleistocene, the $\delta^{18}O_{O2}$ has progressively decreased from about −0.2 to 1.3‰ as a result of disappearance of the Laurentide and Eurasian ice sheets (Bender et al., 1999).

Gases entrapped in intrasedimental ice

In contrast to atmospheric gases in occluded firn air, the molar gas ratios in intrasedimental ice formations, which include pore, wedge, segregated and intrusive ice, are expected to be different from atmospheric ratios due to the different solubilities of the gases in water. Under equilibrium conditions, gases dissolve in water according to their Henry's Law solubility constant, K_H:

$$K_{H_{gas}} = \frac{m_{gas}}{P_{gas}} \quad (1)$$

Henry's constant (mol kg^{-1} atm^{-1}) is a temperature-dependent factor relating the dissolved concentration, m_{gas} in moles per kg of water with partial pressure, P_{gas}, of the gas (atm). The partial pressure of a gas is its fractional contribution to the total gas pressure P_{total}, and it is calculated as its molar fraction multiplied by the total gas pressure:

$$P_{gas} = \frac{mols_{gas}}{mols_{total}} \cdot P_{total}(atm) \quad (2)$$

The concentration of dissolved gas in water is often expressed volumetrically to be consistent with the analytical method used. The units are then $cc_{gas\text{-}STP}/cc_{water}$, where $cc_{gas\text{-}STP}$ is the cm^3 volume occupied by the moles of the gas at standard temperature

https://doi.org/10.1016/j.yqres.2007.05.003 Published online by Cambridge University Press

and pressure (STP = 273.16K and 1 atmosphere). The proportionality constant for gas solubility expressed as a volume at STP rather than as mole fraction is the Bunsen coefficient, B_0, which is equal to K_H RT_K.

Using the Bunsen coefficient (Benson and Krause, 1980, 1984) and Henry's constant for O_2, N_2 and Ar (CRC, 1988; Andrews, 1992), the equilibrium gas concentration in water at STP was calculated. The higher solubility of argon in water results in O_2/Ar and N_2/Ar ratios of 20.83 and 35.50, respectively, which are lower than for atmospheric ratios. The isotopic composition of N_2 and O_2 dissolved in fresh water also differs from their values in air. Kendall and Aravena (2000) showed that $\delta^{15}N$ of dissolved N_2 is 1‰. For oxygen, fractionation during dissolution is on the order of 0.7‰. Therefore, intrasedimental ice is expected to have a different relative abundance of O_2, N_2 and Ar from firnified glacier ice, but similar $\delta^{18}O_{O2}$ and $\delta^{15}N_{N2}$ as fractionation is not greatly affected by dissolution.

Measurement of relative concentration and stable isotope composition of gases in ice

Two main steps are involved in the measurement of the relative abundance and stable isotope composition of gases entrapped in ice: the extraction of gases from the ice, and their analysis by either continuous flow or dual inlet on an isotope-ratio mass spectrometer. The extraction of gases can be accomplished following any of three main techniques. A dry extraction technique is commonly used to analyze for CO_2 gas because the potential CO_2 contamination by dust particles containing carbonates in the ice could modify the concentration and $\delta^{13}C$ composition of CO_2 if the ice were melted (Zumbrunn et al., 1982; Sowers et al., 1997). Following the dry extraction technique, a large sample of ice (~100 g) is crushed in a stainless steel cylinder to release the gases and the CO_2 is cryogenically separated from the released gases using a series of liquid nitrogen traps. However, a problem with this technique is that not all gases may be recovered during the crushing of the ice. Sublimation of the ice is used to solve this limitation, but sublimating the ice is very time-consuming (Henderson, 2000).

For gases, such as O_2, N_2 and Ar, a wet extraction technique is used because dissolved carbonate dust is not an additional contamination source. In this technique, a relatively small quantity of ice (<50 g) is melted and refrozen from the bottom, forcing the dissolved gases out of the water, which are then condensed in a stainless steel sample tube immersed in liquid helium.

The extraction procedure followed in this study was modified from the wet-extraction method developed by Sowers et al. (1997) because it allows the release and recovery of all gas trapped in the ice (recovery greater than 99%). Air collected outside the laboratory building was used as the standard reference gas and yielded average O_2/Ar and N_2/Ar ratios of 22.43±0.58 and 83.60±7.87, respectively, similar to the theoretical atmospheric composition. The stable isotope results are presented using the δ-notation representing the parts per thousand differences for $^{18}O/^{16}O$ or $^{15}N/^{14}N$ from the standard reference gas. The $\delta^{18}O_{O2}$ and $\delta^{15}N_{N2}$ values averaged −0.01±0.29‰ and −0.01±0.23‰, respectively, indicating that the method is precise and reproducible. The complete description of the method used in this study is presented in Appendix A.

Site descriptions and sampling techniques

Various ice types were collected to measure the relative abundance of O_2, N_2 and Ar, as well as $\delta^{18}O_{O2}$ and $\delta^{15}N_{N2}$ of the air entrapped in the ice (Fig. 1). Glacier ice samples were collected from the Agassiz Ice Cap, Ellesmere Island, Nunavut (NU) and the Barnes Ice Cap, Baffin Island (NU). Samples of aufeis ice were collected from the Firth River aufeis located in the northern Yukon Territory (YT) and massive ground ice samples of segregated-intrusive origins were collected from the Aklavik Plateau, Northwest Territories (NT), and Nunavik, Québec (QC).

Glacier ice: Agassiz Ice Cap, Ellesmere Island, Nunavut

Agassiz Ice Cap (80°40′N; 73°30′W; 1730 m a.s.l.) is located on Ellesmere Island (NU) and covers a surface area of approximately 16,000 km^2. Ice cores have provided records of stable oxygen isotope ratios (Fisher et al., 1983; Fisher and Koerner, 1994; Fisher et al., 1995), ice-melt stratigraphy (Koerner and Fisher, 1990), pH and conductivity (Koerner and Fisher, 1982; Barrie et al., 1985), pollen deposition (Bourgeois et al., 2000) and solid electrical conductivity (Zheng et al., 1998). The ice core used in this study was obtained in the spring of 1993 using an electromechanical drill (Zheng et al., 1998). The ice core was stored in plastic lay-flat tubes inside core boxes and cooled at −45 °C several days before shipment to Ottawa. Once in Ottawa, the ice cores were kept at −10 °C in the Geological Survey of Canada Snow and Ice Core Laboratory. The samples analyzed for relative concentration of O_2, N_2 and Ar and $\delta^{18}O_{O2}$ and $\delta^{15}N_{N2}$ values are from the 107- to 112-m depth, corresponding to the Pleistocene–Holocene transition period.

Glacier ice: Barnes Ice Cap, Baffin Island, Nunavut

Barnes Ice Cap (69°39′N; 72°39′W; 400 m a.s.l.) is located on central Baffin Island (NU) and is the remnant Foxe Dome of the Laurentide Ice Sheet. In the summer 2000, ice block samples were collected about 20 cm below the surface after scrapping off any slush or snow to minimize possible mixing with liquid or refrozen runoff using an ice chisel from an ~2-km transect where Pleistocene and Holocene-age ice strata outcrop on the margin of the ice cap (Zdanowicz et al., 2002). Based on their stratigraphic position in relation to the $\delta^{18}O$ profile measured across the ice cap margin, the Barnes Ice Cap samples can be separated into Pleistocene and Holocene age groups. The late Pleistocene (Wisconsin-age) ice strata is characterized by low $\delta^{18}O$ values (−41 to −31‰), whereas the Holocene-age ice displays higher $\delta^{18}O$ values (up to −20‰) (Fig. 4). However, there is an anomaly in the Pleistocene-age ice zone, with higher $\delta^{18}O$ values (up to −26‰). This anomaly was interpreted as being a possible recumbent fold or some other structural mixing between the Holocene and Pleistocene ice at the margin of the ice cap (Zdanowicz et al., 2002). Nine samples were analyzed across the Pleistocene-age strata and three samples from the

https://doi.org/10.1016/j.yqres.2007.05.003 Published online by Cambridge University Press

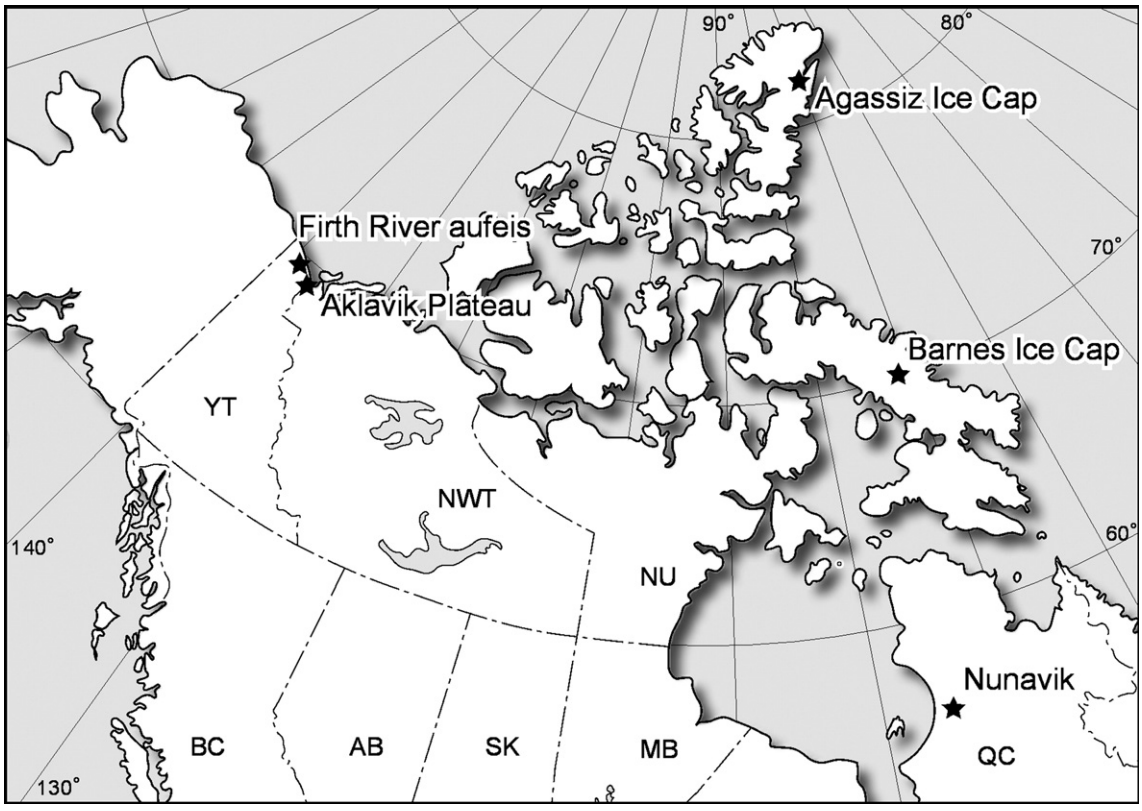

Figure 1. Map showing location of sampled sites in the Canadian Arctic.

anomalous zone to determine the relative concentration of O_2, N_2 and Ar as well as the $\delta^{18}O_{O2}$ and $\delta^{15}N_{N2}$ values.

Aufeis ice: Firth River aufeis, northern Yukon Territory

Aufeis (river icings) are sheet-like masses of horizontally layered ice that accumulate on river channels in permafrost regions by the freezing of successive overflows of perennial groundwater-fed springs upon exposure to cold air. The sampled aufeis, which covers a surface area of 31.5 km^2, is located on the upper Firth River in the British Mountains, northern Yukon Territory (Fig. 2). Samples of aufeis ice were collected in spring 1993 using a hand-held ice auger. Samples were kept frozen and shipped to Ottawa in a thermally insulated box. The cores were sub-sampled and analyzed for their $\delta^{18}O$ and δD values (Clark and Lauriol, 1997), with the core slabs archived at −20 °C. A stable oxygen isotope profile from a core obtained on the Firth River aufeis shows Rayleigh-type trends across the rhythmic ice layering, suggesting that the aggradation of the aufeis occurs under closed-system conditions (Clark and Lauriol, 1997). Eight samples of aufeis ice were analyzed for O_2/Ar and N_2/Ar molar ratios, as well as $\delta^{18}O_{O2}$ and $\delta^{15}N_{N2}$ values, across the vertical profile.

Massive segregated-intrusive ground ice: Aklavik Plateau, Northwest Territories

On the Aklavik Plateau (68°05N; 139°40W; 300 m a.s.l.), Richardson Mountains (NT), extensive beds of debris-rich ice overlain by an icy diamicton were found exposed in the headwalls of retrogressive thaw flows (Fig. 3) (Lacelle et al., 2004). The exposed massive ground ice was sampled in summer 2000 using an ice chisel. As sampling took place during the thaw season, approximately 10 cm of ice was removed from the surface to minimize possible mixing with liquid and refrozen runoff. The ice blocks were kept frozen in a thermally insulated box during transport back to Ottawa. The debris-rich ice is characterized by low $\delta^{18}O$ values (−30 to −27‰) and a CO_2 concentration similar to biogenically produced CO_2 (up to 9 times greater than atmospheric values). Based on these results, Lacelle et al. (2004) suggested that the debris-rich ice consisted of segregated-intrusive ice that was fed by subglacial meltwater moving through a proglacial talik (unfrozen zone in an area of permafrost) under high artesian pressure during the retreat of the Laurentide Ice Sheet and subsequently formed during aggradation of permafrost upon exposure to cold temperatures. Only two samples from the late Pleistocene massive segregated-intrusive ice unit were analyzed for their relative O_2, N_2 and Ar concentration as well as $\delta^{18}O_{O2}$ and $\delta^{15}N_{N2}$ values because of the difficult sampling conditions and in keeping and transporting frozen ice samples during peak summer conditions.

Massive segregated ground ice: Nunavik, Québec

An experimental research site has been established near Umiujap in Nunavik (northern Québec) by the Centre d'Etudes Nordiques (Université Laval) to monitor permafrost and frost mounds dynamics. The study area is located in a valley filled by

https://doi.org/10.1016/j.yqres.2007.05.003 Published online by Cambridge University Press

Figure 2. Photograph of the Firth River aufeis, northern Yukon Territory.

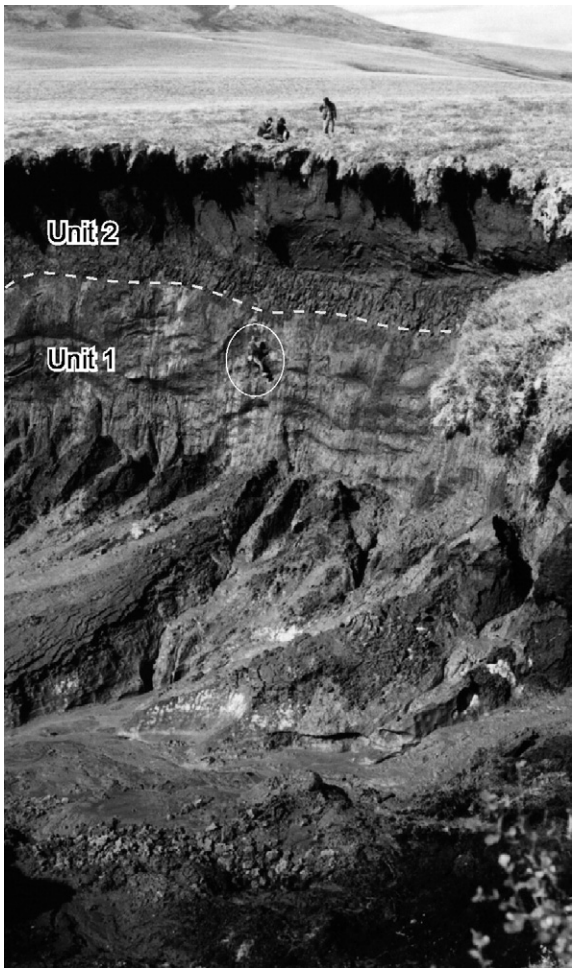

Figure 3. Photograph of late Pleistocene massive segregated-intrusive ice of subglacial meltwater origin exposed in the headwall of a retrogressive thaw flow on the Aklavik Plateau, NWT.

post-glacial marine silts deposited by the Tyrell Sea about 6000 yr ago (Lajeunesse and Allard, 2003). The aggradation of permafrost at this site took place about 3200 yr ago and led to the development of numerous frost mounds, including palsas (Allard et al., 1987). Two late Holocene palsas were sampled in summer 2003 using a portable corer. The palsas measure approximately 50 m wide and 2.5 m high, and their surface is covered by sand. The internal structure of the palsas is composed of ice layers varying in thickness from a few centimeters to 35 cm and separated by glaciomarine silts. Only three samples of late Holocene massive segregated ice were analyzed for occluded gas content, due to the relatively small amount of ice recovered by coring the palsas and the logistical complications in returning frozen samples in summer.

Results

Molar ratios

Glacier ice and intrasedimental ice can be distinguished based on their O_2/Ar and N_2/Ar ratios (Fig. 4). The Pleistocene-age ice samples from Agassiz Ice Cap have O_2/Ar and N_2/Ar ratios averaging 22.54±0.48 and 87.04±2.81, respectively. The molar gas ratios of the Pleistocene-age ice from Barnes Ice Cap averages 18.87±1.03 for O_2/Ar and 78.42±2.23 for N_2/Ar, whereas those obtained from the anomalous zone are 20.00±0.31 and 76.76±0.52, respectively. The molar gas ratios of the Barnes Ice Cap samples are slightly different from the atmospheric ratios. The molar gas ratios obtained from intrasedimental ice are, by contrast, significantly lower than the atmospheric ratios. The late Pleistocene massive segregated-intrusive ice collected on the Aklavik Plateau yielded O_2/Ar and N_2/Ar ratios of 11.42 and 75.92, respectively, whereas the late Holocene massive segregated ground ice samples collected from the one palsa in

https://doi.org/10.1016/j.yqres.2007.05.003 Published online by Cambridge University Press

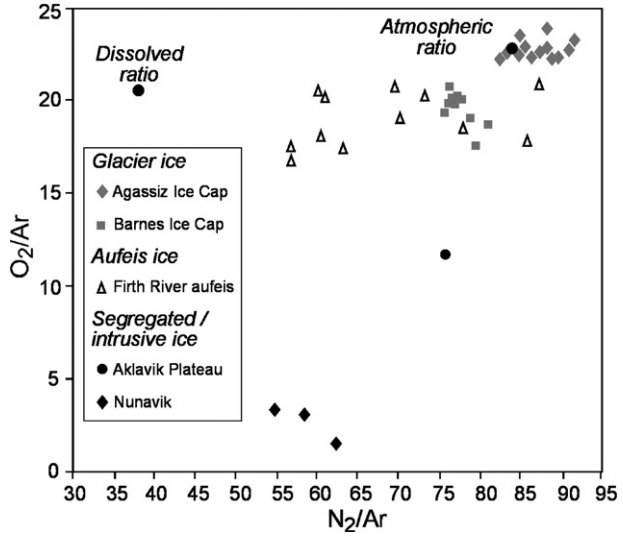

Figure 4. Summary of molar gas ratios (O_2/Ar and N_2/Ar) of air entrapped in glacier ice (Agassiz and Barnes ice caps), aufeis ice (Firth River aufeis) and intrasedimental ice (late Pleistocene massive segregated-intrusive ice and Holocene segregated ice).

Nunavik provided average O_2/Ar and N_2/Ar ratios of 3.00±0.17 and 56.55±2.49, respectively. The other palsa provided similar molar ratios, with a value of 1.34 for N_2/Ar and 62.21 for O_2/Ar. The molar gas ratios of the aufeis, with average O_2/Ar and N_2/Ar values of 18.79±1.49 and 68.45±10.66, respectively, fall between the atmospheric and theoretical dissolved gas molar ratios, indicative of dissolved gases in water with a strong atmospheric signal. This was expected given that the aufeis forms from perennial groundwater-fed springs and also receives an important contribution of snow accumulating onto its surface, forming a mixture of slushy ice prior to freeze-up (e.g., Heldmann et al., 2005). The complete results and statistical summary of the molar gas ratios of the various ice formations are presented in Appendix B (Supplementary Table 1).

Stable O–N isotope ratios

There is some variability in the $\delta^{18}O_{O2}$ and $\delta^{15}N_{N2}$ of the various ice types (Fig. 5). The $\delta^{18}O_{O2}$ and $\delta^{15}N_{N2}$ values of the occluded gases in the Agassiz Ice Cap samples average 1.35±0.94 and 0.57±0.34, respectively, which are slightly higher than atmospheric values. In the Barnes Ice Cap and aufeis ice samples, the $\delta^{18}O_{O2}$ and $\delta^{15}N_{N2}$ composition of occluded gases are similar to atmospheric values. The late Pleistocene massive segregated-intrusive ice from the Aklavik Plateau provided a $\delta^{18}O_{O2}$ and $\delta^{15}N_{N2}$ value of −0.1‰ and −0.9‰, respectively, which is close to the anticipated result for direct dissolution of these gases from air. The late Holocene massive segregated ice from Nunavik yielded $\delta^{18}O_{O2}$ and $\delta^{15}N_{N2}$ values of 2.0±1.3‰ and 0.4±0.1‰, respectively, which are enriched over both the dissolved and atmospheric values. The complete results and statistical summary of the $\delta^{18}O_{O2}$ and $\delta^{15}N_{N2}$ values of the various ice formations are presented in Appendix B (Supplementary Table 2).

Discussion

The comparison of the O_2/Ar, N_2/Ar, $\delta^{18}O_{O2}$ and $\delta^{15}N_{N2}$ values of gases occluded in the various MI/IS bodies, although limited, is instructive and generally supports the theoretical calculations. Despite the considerable variability in $\delta^{18}O_{O2}$ and $\delta^{15}N_{N2}$ values of the various ice formations examined, they offer no characteristic trend to distinguish between glacier and intrasedimental ice (Fig. 5). Rather, the variations are more closely related to *in situ* processes during the formation of the ice. For example, in the case of firnified glacier ice, these modifications include gas partitioning by firn air diffusion and possible diffusion through micro-fractures.

The molar ratios of gases occluded in MI/IS bodies clearly distinguish between glacier ice and intrasedimental ice (Fig. 4). The O_2/Ar and N_2/Ar ratios of glacier ice tend to preserve a signature slightly modified from atmospheric value, whereas the molar gas ratios of intrasedimental ice are significantly modified from atmospheric values due to the dissolution of the gases in water. The measured molar gas ratios in such refrozen samples, however, differ from the calculated values for equilibrium dissolution of gases in water. In the following sections, the processes that can lead to the modification of the molar gas ratios in the glacier ice and intrasedimental ice are discussed.

Variations in molar ratios of glacier ice

The Agassiz Ice Cap O_2/Ar and N_2/Ar ratios are slightly higher than the atmospheric ratios. During the recovery of the ice core, Zheng et al. (1998) observed the presence of micro-fractures within the ice; during the extraction of the gases, the ice was very brittle. Experimental work by Sowers and Bender (1989) indicated that the presence of micro-fractures in the ice could result in the loss of gases that have smaller cross-sectional

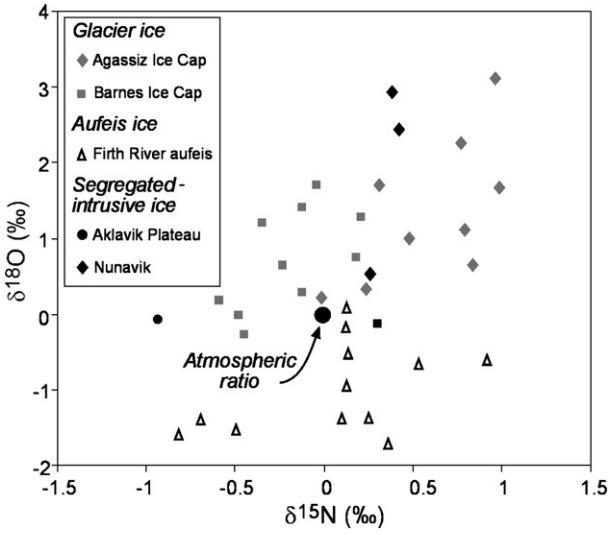

Figure 5. Summary of $\delta^{18}O_{O2\ and}$ $\delta^{15}N_{N2}$ of air entrapped in glacier ice (Agassiz and Barnes ice caps), aufeis ice (Firth River aufeis) and intrasedimental ice (late Pleistocene massive segregated-intrusive ice and Holocene segregated ice).

https://doi.org/10.1016/j.yqres.2007.05.003 Published online by Cambridge University Press

diameter, like Ar, resulting in increased O_2/Ar and N_2/Ar ratios relative to atmospheric values. Consequently, prior to and during pumping of the ice in the extraction vessel, some of the Ar may have been lost, causing a slight increase in the measured O_2/Ar and N_2/Ar ratios.

The molar gas ratios from samples taken across the Pleistocene-age ice strata in the Barnes Ice Cap are slightly lower than the Agassiz Ice Cap and atmospheric values (Fig. 4). A steady-state reconstruction model of the Laurentide Ice Sheet suggests that the Pleistocene-age strata in Barnes Ice Cap originated high up on the ice sheet (Zdanowicz et al., 2002), where temperatures were much colder. The lower O_2/Ar and N_2/Ar ratios in the Barnes Ice Cap may be due to the thermo-gravitational fractionation of heavy gases, such as Ar, relative to lighter gases (e.g., O_2 and N_2) during the occlusion of atmospheric air in the firn (Craig et al., 1988; Sowers et al., 1992).

Variations in molar ratios of intrasedimental ice

For MI/IS bodies generated by the freezing of water, the O_2/Ar and N_2/Ar values can deviate from the theoretical value of gas dissolved at STP due to several physical and biological processes operating in the subsurface. Fig. 6 shows the general pathways for such secondary processes affecting the molar gas ratios of intrasedimental ice formations. The main physical process that can modify the theoretical dissolved molar gas ratios values is the addition of excess atmospheric air. Such a process was clearly observed in the O_2/Ar and N_2/Ar values of the Firth River aufeis. Aufeis ice, which forms during winter by successive overflows of perennial groundwater, also receives a contribution of snow falling onto its surface. Accordingly, the O_2/Ar and N_2/Ar values of the gas entrapped in the ice, which fall between the atmospheric and dissolved ratios, reflect the dissolved gases content in the groundwater and the atmospheric signal originating from air in the snow.

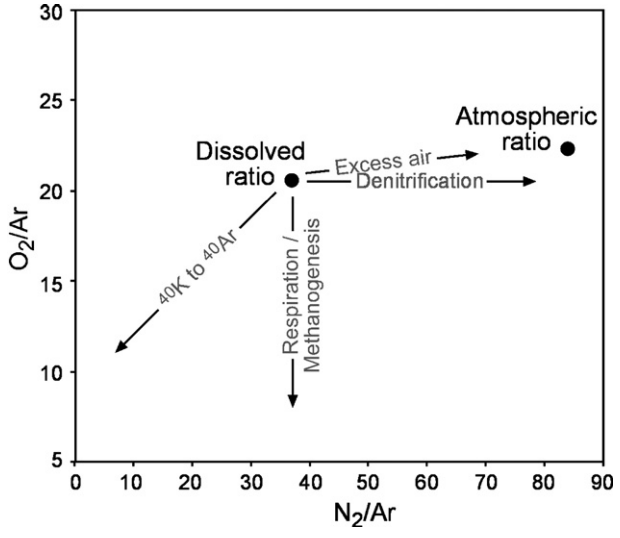

Figure 6. General pathways of processes that can modify the molar gas ratios of intrasedimental ice formations prior to freezing.

The addition of excess air was also observed in the N_2/Ar ratio of the segregated ground ice (palsas). The fine-grained porous media provided by the glaciomarine silts covering the valley floor where the palsas developed are favorable conditions for the entrainment of atmospheric air in the subsurface. The supply of atmospheric air to the subsurface can occur during recharge of the water table from an unsaturated zone, when small air bubbles may become trapped in capillary fringe and forced down below the water table (Heaton and Vogel, 1981). At a certain hydrostatic pressure or depth below the water table, the trapped atmospheric gases will dissolve into the water, thus adding an atmospheric component to the dissolved molar gas ratios. As an example, the N_2/Ar ratios of the segregated ice fall within the range of dissolved gas in fresh water at standard temperature and pressure with approximately 0.05 cc/cc in excess air content.

Known biological reactions that can modify the dissolved molar gas ratios include respiration, methanogenesis and denitrification. The effect of respiration was observed in the O_2/Ar ratio measured in the late Pleistocene segregated-intrusive icy sediments on the Aklavik Plateau. The lower measured ratio relative to the expected dissolved gas molar ratio points to a selective loss of O_2 during bacterial respiration in the groundwater prior to freezing. Lacelle et al. (2004) reported CO_2 concentrations of up to 9 times higher in the ice (128 μg C kg^{-1} ice; $\delta^{13}C_{CO2}$ averaging -21.9 ± 2.1‰) compared to atmospheric values due to microbial respiration, which oxidized organic carbon to CO_2. This microbial effect consequently decreased the amount of O_2 available, and as a result reduced the observed O_2/Ar ratio from its theoretical dissolved value. The effect of respiration was also observed in the O_2/Ar values of the ice mounds in Nunavik. The Nunavik segregated ice formed where *in situ* respiration of buried organics, evident from the elevated CO_2 concentrations and $\delta^{13}C_{CO2}$ values as low as −18‰ in association with trace concentrations of methane in the ice (Calmels, 2005), has reduced available O_2.

The O_2/Ar ratio of the Firth River aufeis, since it receives an important contribution from atmospheric gas (snowfall), is also reduced compared to the theoretical dissolved gas molar ratio. The groundwater circulating in this area are in part associated with the production of biogenic methane, which occurs in the absence of O_2 (Clark and Lauriol, 1997). As argon is non-reactive and would remain unchanged during the residence time of the groundwater circulating through the limestone, the lower O_2/Ar ratio most likely represents a mixture between methanogenic groundwaters and an important contribution from snow accumulating on the surface of the aufeis.

A few other processes, although not observed in the samples analyzed, are capable of modifying the O_2/Ar and N_2/Ar ratios in water-derived ground ice. In environments where NO_3^- is available, denitrification can cause an increase in the N_2/Ar ratio over the theoretical dissolved ratio. Denitrification, which occurs under anoxic conditions, would provide additional N_2 to the groundwater, resulting in higher N_2/Ar ratios. Although the production of N_2 by denitrification can be anticipated, in most northern landscapes there may be insufficient excess of NO_3^- to produce a significant and measurable shift to the N_2/Ar

https://doi.org/10.1016/j.yqres.2007.05.003 Published online by Cambridge University Press

ratio. Finally, under certain conditions, the dissolved concentration of Ar could increase from the initial value due to the accumulation of Ar through the radiogenic decay of ^{40}K (Heaton and Vogel, 1981), which would lower the O_2/Ar and N_2/Ar ratios relative to the theoretical dissolved gas molar ratios.

Conclusion

In theory, analyzing the concentration of the occluded gases within MI/IS bodies should distinguish glacier ice, formed through the process of firn densification, from intrasedimental ice, formed by the freezing of water. To test this, a gas-extraction line that uses liquid helium to isolate atmospheric gases entrapped in ice was constructed based on a design conceived by Sowers and Bender (1989). The new method, which is based on dilution of the gases in helium coupled with analysis using a continuous flow isotope ratio mass spectrometry (IRMS), allows for rapid analysis of the concentration of the gases and their stable isotope ratios on smaller quantities of samples compared to dual-inlet procedure. The results, although obtained on a limited number of samples, indicate that the $\delta^{18}O_{O2}$ and $\delta^{15}N_{N2}$ composition of the various ice formations examined offer no characteristic trend to distinguish between glacier and intrasedimental ice. However, the O_2/Ar and N_2/Ar ratios of gases occluded in MI/IS bodies are able to distinguish clearly between glacier ice and intrasedimental ice. The O_2/Ar and N_2/Ar ratios of glacier ice preserved a signature slightly modified from atmospheric value, whereas the molar gas ratios of intrasedimental ice are significantly modified from atmospheric values due to the dissolution of the gases in water. This novel approach provides an efficient tool for discriminating between buried glacier and intrasedimental ice.

Acknowledgments

This project was supported by Natural Sciences and Engineering Research Council of Canada (NSERC) discovery grants to I.D. Clark and B. Lauriol and by a Northern Scientific Training Program (NSTP) grant to D. Lacelle. We would like to thank W. Abdi, P. Middlestead and G. St-Jean (G.G. Hatch Laboratory, University of Ottawa) for their technical assistance in the development of the gas extraction line and T. Sowers who invited us to visit his lab in Pennsylvania. The manuscript benefited from the constructive comments made by two anonymous reviewers and J. Quade (associate editor).

Appendix A. Description of wet extraction technique

To extract the gases occluded in ice, approximately 50 g of ice is placed inside a round bottom glass vessel that is immersed in a cold ethanol bath (−80 °C) and pumped under vacuum conditions for 30 min to remove possible gas contamination. The ice is then melted by submerging the glass vessel in warm water, which releases the gases trapped in the ice. The ice is then frozen using the cold ethanol bath (−30 °C) from the bottom, leaving O_2, N_2 and Ar exsolved. The released gases are then condensed into a stainless steel sample tube immersed in liquid helium. After a second melt/freeze condensation cycle, the stainless steel tube is closed off and brought to room temperature. Sample gas is then expanded into a high-vacuum, low-volume transfer loop and mixed with ultrapure He gas. An aliquot of this mixture is then transferred into a glass septum vial and analyzed for the gas ratios and isotopic content of O_2, N_2 and Ar through a GasBench II interfaced to a Finnigan Mat Delta^{plus} XP isotope ratio mass spectrometer with a special eight-collector assembly. Because N_2 uses the same collectors as O_2, a peak jump was needed to measure N_2. Ar, N_2 and O_2 reference gases are also measured every time for stable isotope ratio measurements. The stable isotope results are presented using the δ-notation representing the parts per thousand differences for $^{18}O/^{16}O$ or $^{15}N/^{14}N$ from a standard reference gas, consisting of atmospheric air sampled outside the laboratory building. The analytical precision of $\delta^{18}O_{O2}$ and $\delta^{15}N_{N2}$ is ±0.67 and ±0.54, respectively.

To verify the background gas levels in the extraction and transfer lines, leak checks were performed routinely by closing the valve connecting the manifold to the pump and verifying that the Pirani gauge remained constant and below 10^{-4} mTorr. A blank test was performed to verify the background level of gases on the extraction line and in the gas transfer line from the stainless steel tube to the glass septum vial used for analysis on the mass spectrometer.

To test the accuracy and precision of the method, a compressed air standard and compressed air in degassed ice were analyzed. The compressed air standard was introduced in degassed ice within the glass extraction vessel. This was done by introducing a few fabricated ice cubes in the glass vessel and extracting the gases by a series of two melt/freeze condensation cycles. Afterwards, the compressed air was introduced in the line and an aliquot was trapped in the glass extraction vessel. The results show that there is a difference in the $\delta^{18}O_{O2}$ and $\delta^{15}N$ values between the compressed air and the compressed air in degassed ice (Appendix B, Supplementary Table 3). The $\delta^{18}O_{O2}$ and $\delta^{15}N$ values of compressed air in degassed ice average −6.65±0.08‰ and 0.47±0.13‰, respectively, whereas the $\delta^{18}O_{O2}$ and $\delta^{15}N$ values of compressed air average −10.75±0.44‰ and 0.83± 0.02‰, respectively. This difference is due to the method of introducing the compressed gas into the vessel. Since the temperature of the vessel is at ∼−100 °C during the injection of the compressed gas, a thermo-fractionation of the isotopes is induced as the heavier isotopes of oxygen tend to accumulate at the colder temperature, producing a higher ratio. Since O_2 has a smaller diameter than N_2, it diffuses faster, which is why the difference is more noticeable in $\delta^{18}O_{O2}$ (Craig et al., 1988). The values of $\delta^{15}N$ are too close to discern a difference between compressed air and compressed air introduced in degassed ice.

Finally, the air collected outside the laboratory building, which is used as the standard reference gas, was measured nine times to verify the reproducibility of the data. The average molar ratio O_2/Ar and N_2/Ar are 22.43±0.58 and 83.60±7.87, respectively, very similar to the theoretical atmospheric composition. The $\delta^{18}O_{O2}$ and $\delta^{15}N_{N2}$ values average −0.01±0.29‰ and −0.01±0.23‰, respectively (Appendix B, Supplementary Table 4).

https://doi.org/10.1016/j.yqres.2007.05.003 Published online by Cambridge University Press

Appendix B. Supplementary data

Supplementary data associated with this article can be found, in the online version, at doi:10.1016/j.yqres.2007.05.003.

References

Andrews, J.N., 1992. Mechanisms for noble gas dissolution by groundwater. Isotopes of noble gases as tracers in environmental studies. International Atomic Energy Agency, Vienna 87–109.

Allard, M., Seguin, M.L., Levesque, R., 1987. Palsas and mineral frost mounds in northern Quebec. Proceeding 1st Conference International Geomorphology, vol. 2, pp. 285–309.

Associated Committee on Geotechnical Research (ACGR), 1988. Glossary of permafrost and related ground ice terms. Permafrost Subcommittee, National Research Council of Canada Technical Memorandum 142, 156p.

Astakhov, V.I., 1986. Geological conditions for the burial of Pleistocene glacier ice on the Yenisey. Polar Geography and Geology 10, 286–295.

Arnaud, L., Barnola, J.-M., Duval, P., 2000. Physical modeling of the densification of snow/firn and ice in the upper part of polar ice sheets. In: Hondoh, T. (Ed.), Physics of Ice Core Records. Sapporo, pp. 285–305.

Barnola, J.M., Pimienta, P., Raynaud, D., Korotkevich, Y.S., 1991. CO_2 climate relationship as deduced from the Vostok ice core: a reexamination based on new measurements and on reevaluation of the air dating. Tellus 43, 83–90.

Barrie, L.A., Fisher, D.A., Koerner, R.M., 1985. Twentieth century trends in arctic air pollution revealed by conductivity and acidity observations in snow and ice in the Canadian High Arctic. Atmospheric Environment 19, 2055–2063.

Bender, M., Sowers, T., Dickson, M.L., Orchardo, J., Grootes, P., Mayewski, P.A., Meese, D.A., 1994. Climate correlations between Greenland and Antarctica during the past 100,000 years. Nature 372, 663–666.

Bender, M., Malaize, B., Orchardo, J., Sowers, T., Jouzel, J., 1999. High precision correlations of Greenland and Antarctic ice core records over the last 100 kyr. In: Clark, P.U., Webb, R., Keigwin, L. (Eds.), Mechanisms of Global Climate Change at Millennial Timescales. American Geophysical Union, Washington, DC, pp. 149–164.

Benson, B.B., Krause Jr., D., 1980. The concentration and isotopic fractionation of gases dissolved in freshwater in equilibrium with the atmosphere. Limnology and Oceanography 25, 662–671.

Benson, B.B., Krause Jr., D., 1984. The concentration and isotopic fractionation of oxygen dissolved in freshwater and seawater in equilibrium with the atmosphere. Limnology and Oceanography 29, 632–662.

Bourgeois, J.C., Koerner, R.M., Gajewski, K., Fisher, D.A., 2000. A Holocene ice-core pollen record from Ellesmere Island, Nunavut, Canada. Quaternary Research 54, 275–283.

Burn, C.R., Michel, F.A., Smith, M.W., 1986. Stratigraphic, isotopic, and mineralogical evidence for an early Holocene thaw unconformity at Mayo Yukon Territory. Canadian Journal of Earth Sciences 23, 794–803.

Caillon, N., Severinghaus, J.P., Jouzel, J., Barnola, J., Kang, J., Lipenkov, V.Y., 2003. Timing of atmospheric CO_2 and Antarctic temperature changes across termination III. Science 299, 1728–1731.

Calmels, F. 2005. Genèse et structure du pergélisol: Étude de formes périglaciaires de soulèvement au gel au Nunavik (Québec nordique), Canada. Unpublished PhD thesis, Université Laval, St-Foy, Québec, Canada.

Clark, I.D., Lauriol, B., 1997. Aufeis of the Firth River Basin, Northern Yukon, Canada: insights into permafrost hydrogeology and karst. Arctic and Alpine Research 29, 240–252.

Clark, I.D., Henderson, L., Chappellaz, J., Fisher, D., Koerner, R., Worthy, D.E.J., Kotzer, T., Norman, A.-L., Barnola, J.-M., 2007. CO_2 isotopes as tracers of firn air diffusion and age in an Arctic ice cap with summer melting, Devon Island, Canada. Journal of Geophysical Research 112, doi:10.1029/2006JDS007471.

Craig, H., Horibe, Y., Sower, T., 1988. Gravitational Separation of gases and isotopes in polar ice caps. Science 1675–1678.

CRC handbook of chemistry and physics, 1988. Weast, R.C. (Ed.), The chemical rubber Co., Boca Raton.

Dyke, A.S., Savelle, J.M., 2000. Major end moraines of Younger Dryas age on Wollaston Peninsula, Victoria Island, Canadian Arctic: implications for paleoclimate and for formation of hummocky moraine. Canadian Journal of Earth Sciences 37, 601–619.

Fisher, D.A., Koerner, R.M., 1994. Signal and noise in four ice-core records from the Agassiz Ice Cap, Ellesmere Island, Canada: details of the last millennium for stable isotopes, melt and solid conductivity. The Holocene 4, 113–120.

Fisher, D.A., Koerner, R.M., Reeh, N., 1995. Holocene climatic records from Agassiz Ice Cap, Ellesmere Island, NWT, Canada. The Holocene 5, 19–24.

Fisher, D.A., Koerner, R.M., Paterson, W.S.B., Dansgaard, W., Gundestrup, N., Reeh, N., 1983. Effect of wind scouring on climatic records from ice-core oxygen-isotope profiles. Nature 301, 205–209.

French, H.M., Pollard, W.H., 1986. Ground-ice investigations, Klondike District, Yukon Territory. Canadian Journal of Earth Sciences 23, 550–560.

French, H.M., Harry, D.G., 1990. Observations on buried glacier ice and massive segregated ice, western Arctic coast, Canada. Permafrost and Periglacial Processes 1, 31–43.

Harry, D.G., French, H.M., Pollard, W.H., 1988. Massive ground ice and ice-cored terrain near Sabine Point, Yukon Coastal Plain. Canadian Journal of Earth Sciences 25, 1846–1856.

Hattori, A., 1983. Denitrification and dissimilatory nitrate reduction. In: Carpenter, E.J., Capone, D.G. (Eds.), Nitrogen in the Marine Environment. Academic Press, San Diego, pp. 141–191.

Heaton, T.H.E., Vogel, J.C., 1981. "Excess air" in groundwater. Journal of Hydrology 50, 201–216.

Heldmann, J.L., Pollard, W.H., McKay, C.P., Andersen, D.T., Toon, O.B., 2005. Annual development cycle of an icing deposit and associated perennial spring activity on Axel Heiberg Island, Canadian High Arctic. Arctic, Antarctic and Alpine Research 37, 127–135.

Henderson, L., 2000. The CO_2 record in firn air and melt layer ice, Devon Island Ice Cap, Nunavut. Unpublished MSc. thesis, University of Ottawa, Ottawa, ON, Canada.

Kaplyanskaya, F.A., Tarnogradski, V.D., 1986. Remnants of the Pleistocene ice sheets in the permafrost zone as an object for paleoglaciological research. Polar Geography and Geology 10, 257–266.

Kendall, C., Aravena, R., 2000. Nitrate isotopes in groundwater systems. In: Cook, P., Herczeg, A.L. (Eds.), Environmental Tracers in Subsurface Hydrology, pp. 261–297.

Koerner, R.M., Fisher, D.A., 1982. Acid snow in the Canadian Arctic. Nature 295, 137–140.

Koerner, R.M., Fisher, D.A., 1990. A record of Holocene summer melt from a Canadian High Arctic ice core. Nature 343, 630–631.

Lacelle, D., Bjornson, J., Lauriol, B., Clark, I.D., Troutet, Y., 2004. Segregated-intrusive ice of subglacial meltwater origin in retrogressive thaw flow headwalls. Richardson Mountains, NWT, Canada. Quaternary Science Reviews 23, 681–696.

Lajeunesse, P., Allard, M., 2003. The Nastapoka drift belt, eastern Hudson Bay: implication of a stillsand of the Quebec-Labrador ice margin in the Tyrell Sea at 8 Ka BP. Canadian Journal of Earth Sciences 40, 65–76.

Landais, A., Barnola, J.M., Kawamura, K., Caillon, N., Delmotte, M., Van Ommen, T., Dreyfus, G., Jouzel, J., Masson-Delmotte, V., Minster, B., Freitag, J., Leuenberger, M., Schwander, J., Huber, C., Etheridge, D., Morgan, V., 2006. Firn-air ä^{15}N in modern polar sites and glacial–interglacial ice: a model-data mismatch during glacial periods in Antarctica? Quaternary Science Reviews 25, 49–62.

Leibman, M.O., 1996. Results of chemical testing for various types of water and ice, Yamal Peninsula, Russia. Permafrost and Periglacial Processes 7, 287–296.

Lorrain, R.D., Demeur, P., 1985. Isotopic evidence for relic Pleistocene glacier ice on Victoria Island Canadian Arctic Archipelago. Arctic and Alpine Research 17, 89–98.

Mariotti, A., 1983. Atmospheric nitrogen is a reliable standard for natural ^{15}N abundance measurements. Nature 303, 685–687.

Mackay, J.R., 1966. Segregated epigenetic ice and slumps in permafrost, Mackenzie Delta area, N.W.T. Geographical Bulletin 8, 59–80.

Mackay, J.R., 1971. The origin of massive icy beds in permafrost, western Arctic, Canada. Science 8, 397–422.

https://doi.org/10.1016/j.yqres.2007.05.003 Published online by Cambridge University Press

Mackay, J.R., Dallimore, S.R., 1992. Massive ice of the Tuktoyaktuk area, western Arctic coast, Canada. Canadian Journal of Earth Sciences 29, 1235–1249.

Moorman, B.J., Michel, F.A., Wilson, A.T., 1998. The development of tabular massive ground ice at Peninsula Points, N.W.T., Canada. Proceeding, 7th International Conference on Permafrost, Yellowknife, Canada. Collection Nordicana, vol. 55, pp. 757–762.

Murton, J.B., 2005. Ground-ice stratigraphy and formation at North Head, Tuktoyaktuk Coastlands, western Arctic Canada: a product of glacier-permafrost interactions. Permafrost and Periglacial Processes 16, 31–50.

Murton, J.B., French, H.M., 1994. Cryostructures in permafrost, Tuktoyaktuk Coastlands, western Arctic Canada. Canadian Journal of Earth Sciences 31, 737–747.

Murton, J.B., Waller, R.I., Hart, J.K., Whiteman, C.A., Pollard, W.H., Clark, I.D., 2004. Stratigraphy and glaciotectonic structures of permafrost deformed beneath the northwest margin of the Laurentide ice sheet, Tuktoyaktuk Coastlands, Canada. Journal of Glaciology 50, 399–412.

Murton, J.B., Whiteman, C.A., Waller, R.I., Pollard, W., Clark, I.D., Dallimore, S.R., 2005. Basal ice facies and supraglacial melt-out till of the Laurentide Ice Sheet, Tuktoyaktuk Coastlands, western Arctic Canada. Quaternary Science Reviews 24, 681–708.

Petrenko, V., Severinghaus, J.P., Brook, E.J., Reeh, N., Schaefer, H., 2006. Gas records from the West Greenland ice margin covering the last glacial termination: a horizontal ice core. Quaternary Science Reviews 25, 865–875.

Pollard, W.H., 1991. Observations on massive ground ice on Fosheim Peninsula, Ellesmere Island, Northwest Territories. Current Research, Part E. Geological Survey of Canada 91-1E, 223–231.

Rampton, V.N., 1988. Origin of massive ground ice on Tuktoyaktuk Peninsula, Northwest Territories, Canada: a review of stratigraphic and geomorphic evidence. Fifth International Conference Proceedings, vol. 1. Tapir, Trondheim, pp. 850–855.

Schwander, J., 1996. Gas diffusion in firn. In: Wolfe, E.W., Bales, R.C. (Eds.), Chemical Exchange Between the Atmosphere and Polar Snow. NATO ASI SERIES, vol. 1, pp. 528–540.

Sowers, T., Bender, M., 1989. Elemental and isotopic composition of occluded O_2 and N_2 in polar ice. Journal of Geophysical Research 94, 5137–5150.

Sowers, T., Bender, M., Raynaud, D., Korotkevich, Y.S., 1992. $\delta^{15}N$ of N_2 in air trapped in polar ice: a tracer of gas transport in the firn and a possible constraint on ice-age gas differences. Journal of Geophysical Research 97, 15683–15697.

Sowers, T., Brook, E., Etheridge, D., Blunier, T., Fuchs, A., Leuenberger, M., Chappellaz, J., Barnola, J.M., Wahlen, M., Deck, B., Weyhenmeyer, C., 1997. An interlaboratory comparison of techniques for extracting and analyzing trapped gases in ice cores. Journal of Geophysical Research 102, 26527–26538.

St-Onge, D.A., McMartin, I., 1995. The Bluenose Lake Moraine, a moraine with a glacier core. Géographie Physique et Quaternaire 53, 287–295.

Zdanowicz, C.M., Fisher, D.A., Clark, I.D., Lacelle, D., 2002. An ice-marginal ($\delta^{18}O$ record from Barnes Ice Cap, Baffin Island, Canada. Annals of Glaciology 35, 145–149.

Zheng, J., Kudo, A., Fisher, D.A., Blake, E.W., Gerasinoff, M., 1998. Solid electrical conductivity (ECM) from four Agassiz ice cores, Ellesmere Island NWT, Canada: high-resolution signal and noise over the last millennium and low-resolution over the Holocene. The Holocene 8, 413–421.

Zumbrunn, R., Neftel, A., Oeschger, H., 1982. CO_2 measurements on 1-cm^3 ice samples with an IR laserspectrometer (IRSL) combined with a new dry extraction device. Earth and Planetary Science Letters 60, 318–324.

https://doi.org/10.1016/j.yqres.2007.05.003 Published online by Cambridge University Press